Efficient photorelease of carbon monoxide from a luminescent tricarbonyl rhenium(i) complex incorporating pyridyl-1,2,4-triazole and phosphine ligands

Ángel Hernández Mejías, Alexandre Poirot, Meriem Rmili, Nadine Leygue, Mariusz Wolff, Nathalie Saffon-Merceron, Eric Benoist, Suzanne Fery-Forgues

Efficient Photorelease of Carbon Monoxide from a Luminescent Tricarbonyl Rhenium(I) Complex Incorporating Pyridyl-1,2,4-triazole and Phosphine Ligands

Ángel D. Hernández Mejías,[a,b,†] Alexandre Poirot,[a,†] Meriem Rmili,[a,c] Nadine Leygue,[a] Mariusz Wolff,[d] Nathalie Saffon-Merceron,[e] Eric Benoist [a] and Suzanne Fery-Forgues *[a]

[a] *SPCMIB, CNRS UMR 5068, Université de Toulouse III Paul Sabatier, 118 route de Narbonne, 31062 Toulouse cedex 9, France. E-mail : sff@chimie.ups-tlse.fr*

[b] *Department of Chemistry, University of Puerto Rico, Río Piedras Campus, PO Box 23346, San Juan, PR 00931-3346, USA*

[c] *Institut National des Sciences Appliquées et de Technologie, Centre Urbain Nord BP 676-1080 Tunis Cedex, Tunisia*

[d] *Universität Wien, Institut für Chemische Katalyse, Währinger Straße 38, 1090 Wien, Austria*

[e] *Service commun RX, Institut de Chimie de Toulouse, ICT- FR2599, Université de Toulouse III Paul Sabatier, 118 route de Narbonne, 31062 Toulouse cedex 9, France*

† Contributed equally to the work.

ABSTRACT

Precise control over the production of carbon monoxide (CO) is essential to exploit the therapeutic potential of this molecule. The development of photoactive CO-releasing materials (PhotoCORMa) is therefore a promising route for future clinical applications. Herein, a tricarbonyl-rhenium(I) complex (**1-TPP**), which incorporates a phosphine moiety as ancilliary ligand for boosting the photochemical reactivity, and a pyridyltriazole bidentate ligand with appended 2-phenylbenzoxazole moiety for the purpose of photoluminescence, was synthesized and characterized from a chemical and crystallographic point of view. Upon irradiation in the near-UV range, complex **1-TPP** underwent fast photoreaction, which was monitored through changes of the UV-vis absorption and phosphorescence spectra. The photoproducts (i.e. the dicarbonyl solvento complex **2** and one CO molecule) were identified using FTIR, ^{1}H NMR and HRMS. The results were interpreted on the basis of DFT/TD-DFT calculations. The effective photochemical release of CO associated with remarkable optical variations (the emitted light passed from green to orange-red) could make **1-TPP** the prototype of new photochemically-active agents, potentially useful for integration in photoCORMa.

INTRODUCTION

The beneficial therapeutic effects of carbon monoxide (CO) are now clearly evident.[1,2] It has been recently established that this endogenously-produced signaling molecule plays a crucial role in immune and anti-inflammatory responses, as well as in vaso-relaxation. It has the capacity to promote graft survival during organ transplantations, treat cardiovascular diseases, induce apoptosis of cancer tissues, and it shows remarkable antimicrobial activity. However, CO gas has been known for a long time for its toxicity, and its implementation in hospital setting raises technical and safety-related issues. The development of photoactive CO releasing molecules (photoCORMs) that serve as benign CO reservoirs and light-triggered delivery systems is therefore of great research interest and has expanded significantly in the last decade.[3-6] However, a fine control of the localization of photoCORMs and precise monitoring

of CO release are of crucial importance for both biological studies and therapeutics, and these issues are far from being resolved.

In comparison with other metal-carbonyl complexes, tricarbonylrhenium complexes are attractive photoCORMs. Although less photoreactive than their manganese analogues,[7-9] they present distinct advantages, such as being generally air- and water-stable, biocompatible, and intrinsically phosphorescent, so that their distribution in cells can be imaged.[10-12] The groups of Ford and Mascharak have independently shown that the photoreaction could also be followed through a change of the phosphorescence properties, so that the compounds hold significant promises as theranostic photoCORMs.[13,14] Their photoreactivity may be modulated by the nature of the phosphine ligand, and they act as multiaction photoactivated anticancer agents in various cell lines.[15] Recently, our group has developed a new class of tricarbonylrhenium complexes in which the bidentate ligand is a pyridinetriazole (pyta) unit with appended phenylbenzoxazole (PBO) moiety, and the ancillary ligand is a chloride ion. These complexes display valuable spectroscopic properties, closely dependent on the isomerism of the organic ligand [16,17] and they seem to be quite lightfast. In the present work, complex **1-Cl** (Scheme 1), the most emissive complex of the reported series, was selected and modified by replacing the chloride ion by a triphenylphosphine unit, with the purpose of increasing CO photolability.[13,18-21] Herein, the synthesis of this new complex **1-TPP** (Scheme 1), its crystallographic characteristics, as well as its spectroscopic and photochemical behaviour are described. Data are supported by TD-DFT calculations. Results showed that the new compound **1-TPP** undergoes photochemical reaction with good efficiency and remarkable changes of the emission properties, making it a very promising photoCORM.

RESULTS AND DISCUSSION

Synthesis and molecular structure

Complex $[Re(CO)_3(L)(Cl)]$ (**1-Cl**) was first reacted with silver triflate in acetonitrile to obtain the acetonitrile-bound complex $[Re(CO)_3(L)(CH_3CN)]^+(OTf)^-$ according to a procedure developed in the group.[22] This intermediate was then reacted with triphenylphosphine to afford the desired complex,[12]

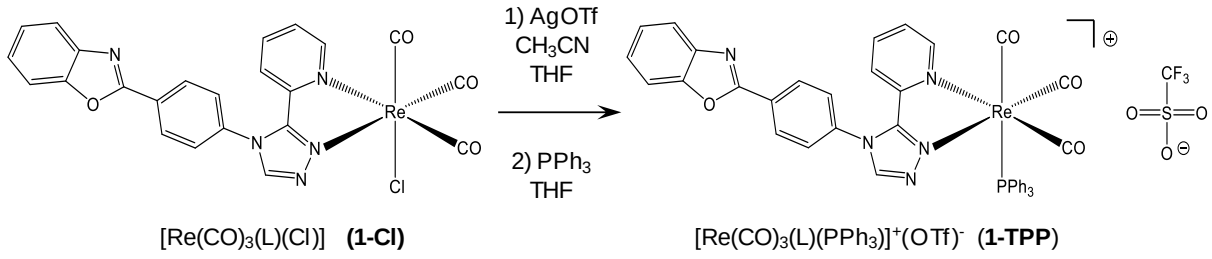

$[Re(CO)_3(L)(Cl)]$ **(1-Cl)** $[Re(CO)_3(L)(PPh_3)]^+(OTf)^-$ (**1-TPP**)

Scheme 1. Synthesis route to complex **1-TPP**.

i.e. $[Re(CO)_3(L)(PPh_3)]^+$ $(OTf)^-$ (**1-TTP**) (Scheme 1). Identifications were made by ^1H and ^{13}C NMR spectroscopy (Fig. S1-S10†), and high resolution mass spectrometry. The ATR infrared spectra of the solid compound **1-TTP** showed the three characteristic ν(CO) stretching bands of the *fac*-$[Re(CO)_3]^+$ unit at ν(CO) = 2044, 1957, 1910 cm^{-1}. The average value was 1970 cm^{-1}, which is significantly lower than for the parent compound (1947 cm^{-1}), indicating that the electron-withdrawing ability of the triphenylphosphine ligand causes a decrease in the electron density at the Re(I) ion.[23]

The slow evaporation of $CDCl_3$ provided large crystals, which underwent rapid degradation once separated from the solution. X-Ray analysis showed that **1-TTP** crystallized as a solvate. Selected crystallographic data are given in the experimental section. As expected, the rhenium ion is coordinated with the three carbonyl groups displayed in a *fac* configuration, two nitrogen atoms N(1) and N(2) of the pyta ligand, and the phosphorous atom P(1) of the triphenylphosphine group (Fig. 1). The examination of bond lengths and angles (Table S1†) showed that the octahedral geometry was slightly more regular than in the parent compound. The Re-C(41) bond facing the ancilliary ligand in **1-TTP** was significantly longer than the corresponding one in **1-Cl** (1.956(7) Å instead of 1.903(8) Å). This lengthening can be attributed to the superior π–accepting capacity of the TPP ligand, which competes with the CO group *trans* to it for the same metal orbitals, and reduces metal-to-CO π–back-bonding.[7,13] The PBO moiety was slightly bent and, remarkably, the phenyl ring formed an angle of 57.5° with the 1,2,4-triazole group, much smaller than the value of 83.3° found for **1-Cl**. Disorder was observed only for the solvent. Only a weak N/O swap was noticed on the PBO unit, contrary to related complexes.[16,17]

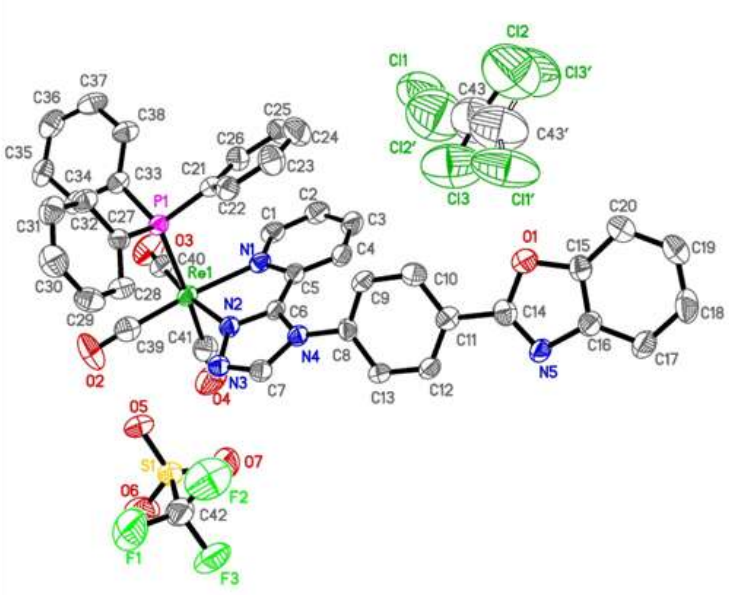

Fig. 1 Molecular view of the solvate of complex **1-TTP**. Hydrogen atoms have been deleted for the sake of clarity.

As for the packing mode, all PBO moieties were displayed on parallel planes, as was also the case for all pyta groups (Fig. 2). The nearest PBO neighbours were distant by ~3.3 Å in the stacking direction, and were anti-parallel to each other (Fig. S11†). The overlap of their aromatic moieties was very small due to both lateral and longitudinal slippages. The pyta moieties were separated from each other by the triflate and by the phenyl groups of the bulky PPh_3 unit. Very few π-π interactions were taking place. Most of them can be found between the pyridine and one phosphine cycle (3.70 Å), and

between the benzo and phenyl groups of stacked molecules (3.80 Å). A few CH···π interactions were also found. The oxygen atoms of the carbonyl groups were involved in hydrogen bonds. Noticeably, the phosphine unit was involved in many CH···OS, CH···N, C···HC, and C···OC short contacts with triflate, benzoxazole, pyta and carbonyl groups, respectively, the H-bond with the shortest distance being N(5)…H(32) (2.57 Å).

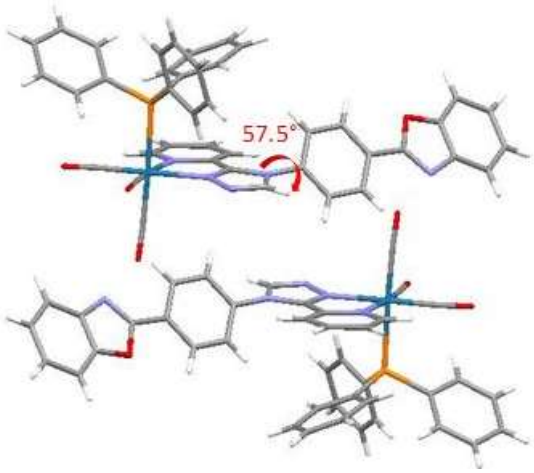

Fig. 2 Unit cell of **1-TTP**. Triflate anions and solvent molecules have been deleted for the sake of clarity.

UV-vis absorption properties and monitoring of the photochemical reaction

The spectroscopic properties of **1-TPP** were determined by recording the absorption spectrum in acetonitrile. An intense band that peaks at 305 nm (ε_{305} = 30600 $M^{-1}cm^{-1}$) was observed, partly overlying a band of moderate intensity between 340 and 400 nm (Fig. 3). Similar spectra were obtained in other organic solvents (Table S2†). No significant changes of the UV-vis absorption spectrum were detected after two months in the dark, which suggests that the complex is chemically stable in acetonitrile solution (Fig. S12†).

To investigate the photochemical behaviour of **1-TPP**, acetonitrile solutions placed in quartz cells were irradiated in two distinct regions of the absorption spectrum, at 300 nm and 350 nm. Results were qualitatively identical. During photolysis, the main band was broadened with a slight absorbance increase, and a distinct band peaking at 402 nm appeared (Fig. 3). The presence of very clear isosbestic points at 271, 314 and 372 nm suggested the formation of only one photoproduct. After complete photolysis, the extinction coefficient of the photoproduct at 402 nm was found to be 4450 $M^{-1}cm^{-1}$, instead of 820 $M^{-1}cm^{-1}$ for **1TPP**. Using Beer-Lambert's law, the photoproduct concentration x was calculated for various irradiation times. The photochemical quantum yield, measured via ferrioxalate actinometry, was found to be 0.10 in aerated solution, and 0.29 in argon-flushed solution for irradiation at 350 nm. The order of the photoreaction was also determined in undegassed solutions. The variation of Log (a-x) *vs* time, with a the initial concentration of **1-TTP**, was linear until 110 s (inset of Fig. 3), indicating a first-order photoreaction with a rate constant value (k), given by the slope, close to 0.033 s^{-1} (1.92 min^{-1}). For irradiation at 300 nm, the k value was 0.45 min^{-1} (Fig. S13†), much lower than for irradiation at 350 nm. Regarding the parent compound **1-Cl**, only a very weak evolution of the

absorption spectrum was detected after 2h of irradiation at 300 nm, showing good photochemical stability (Fig. S14†).

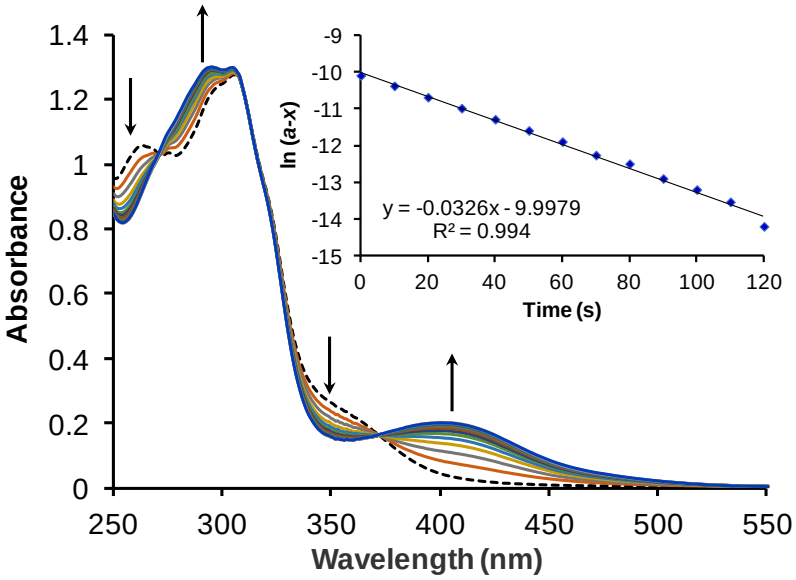

Fig. 3 Monitoring by UV-vis absorption spectroscopy of the photochemical reaction of **1-TPP** in undegassed acetonitrile solution (4.17×10^{-5} M) under irradiation at 350 nm over 3 min. One measurement was collected every 10 s for 120 s, then one measurement was made at 180 s. Initial spectrum in black dashed line. The arrows indicate the evolution of the spectra. Inset: plot of ln(*a*-*x*) *vs* time, with *a* being the initial concentration of **1-TPP** and *x* the concentration of formed photoproduct.

Emission properties

The emission properties of **1-TPP** were first studied in various organic solvents (Table S2†). The complex emitted in the green region. For example, the maximum emission was at 544 nm in acetonitrile (Fig. 4) with moderate quantum yields of 0.033 in aerated solution and ~0.10 in argon-flushed solution. The emission was therefore strongly blue shifted and its efficiency was increased from 3 to 8 fold depending on the solvent, with respect to parent complex **1-Cl**.[17] These changes agree well with those generally reported in the literature when passing from neutral to charged tricarbonyl Re(I) complexes.[23,24] The lifetimes were 399 and 521ns, in undegassed and argon-flushed solutions, respectively. In view of the spectrum position at rather long wavelengths and long luminescence lifetimes, the emission can be assigned to phosphorescence, as is the case for the vast majority of similar complexes.

During the photochemical reaction, the initial green emission of **1-TPP** in acetonitrile became progressively redder and weaker (inset of Fig. 4). The spectra showed the decrease of the band at 544 nm and the appearance of a weak band around 686 nm (Fig. S15†), with formation of an isoemissive point near 692 nm. The quantum yield of the photoproduct can be estimated to be around 5×10^{-3} and the lifetime of the main component was considerably shortened to 33 ns in undegassed solution.

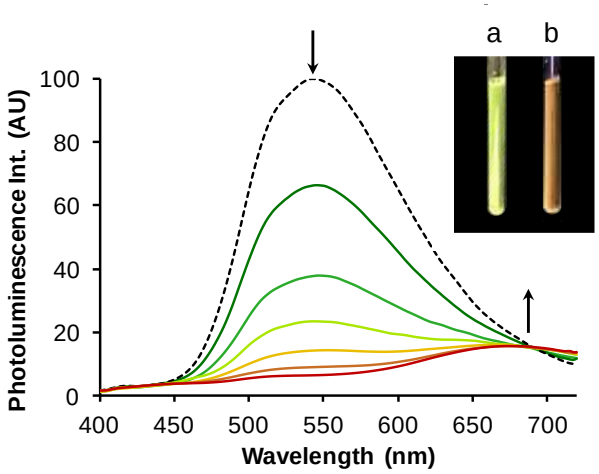

Fig. 4 Monitoring by fluorescence spectroscopy of the photochemical reaction of **1-TPP** in undegassed acetonitrile solution (2.1×10^{-5} M) under irradiation at 350 nm. Scans were obtained every 15 s of irradiation. Initial spectrum (t = 0 s) is represented with the black dashed line. λ_{ex} = 370 nm. Inset: photographs of concentrated solutions (~2.3×10^{-3} M) illuminated by a UV lamp (365 nm) before (a) and after complete photolysis (b).

The emission properties were also studied in the solid state. The microcrystalline powder of **1-TPP** emitted bright yellow light, with maximum at 554 nm (Fig. 5b, left). The photoluminescence quantum yield was 0.018, which is slightly weaker than in solutions, so that no solid-state luminescence enhancement (SLE) was observed contrary to parent compound **1-Cl**.[17] Noticeably, the solid samples of **1-TPP** quickly darkened under the spectrophotometer excitation beam, and the emission faded (Fig. 5b, right), indicating some photochemical instability of this compound in the solid state. Furthermore, when some powder of **1-TPP** was dispersed in water, the formation of bubbles due to photoreaction with the microscope beam (435-450 nm) was observed by optical microscopy, showing fast photoreaction and

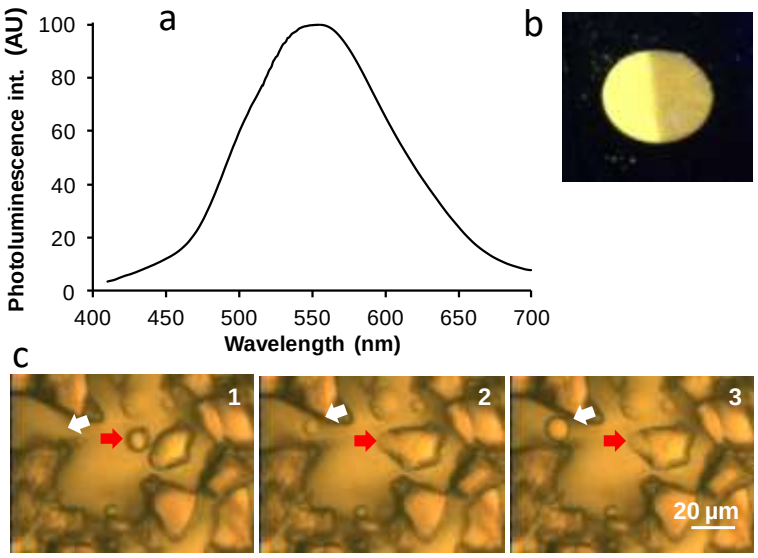

Fig. 5 a) Emission spectrum of complex **1-TPP** in the solid state (pristine powder). λ_{ex} = 380 nm. b) Powder sample observed under a hand-held UV lamp (365 nm), protected from light (left) and illuminated for 15 min by the same UV lamp (right). c) Optical microscopy images of the microcrystalline powder dispersed in water, taken every 15 s. The formation and merging of bubbles due to photolysis by the microscope beam (435-450 nm) are indicated by white and red arrows, respectively.

indicating the gaseous nature of one of the photoproducts (Fig. 5c). Small bubbles were generated in the aqueous medium at distinct nucleation sites, then they grew and merged together to form larger bubbles (Fig. S16†). This type of observation has been reported once for a Mn photoCORM.[25]

Monitoring of the photochemical reaction by additional techniques and identification of the photoproducts

Complementary techniques were used to get a deeper insight into the nature of the photoproducts. The evolution of the ^{1}H NMR spectra in CD_3CN throughout photolysis is given in Fig. 6. It shows that the pyridine protons in the *ortho* and *para* position with respect to the nitrogen atom, i.e. H23 and H25 according to proton numbering in Fig. S17†, were deshielded by 0.22 and 0.07 ppm, respectively, while the signal of the H26 proton in the *meta* position was upfielded by 0.08 ppm. The singlet corresponding to the triazole proton H17 was also shifted to low fields by 0.10 ppm. In contrast, the peaks corresponding to the phosphine protons were almost not affected, as is also the case for the protons of PBO, which is known for its excellent photochemical stability.[26] These results indicate that the photochemical reaction has modified the electronic environment of the pyta moiety, and more precisely the coordination sphere, with an increase of the charge density on the rhenium centre.

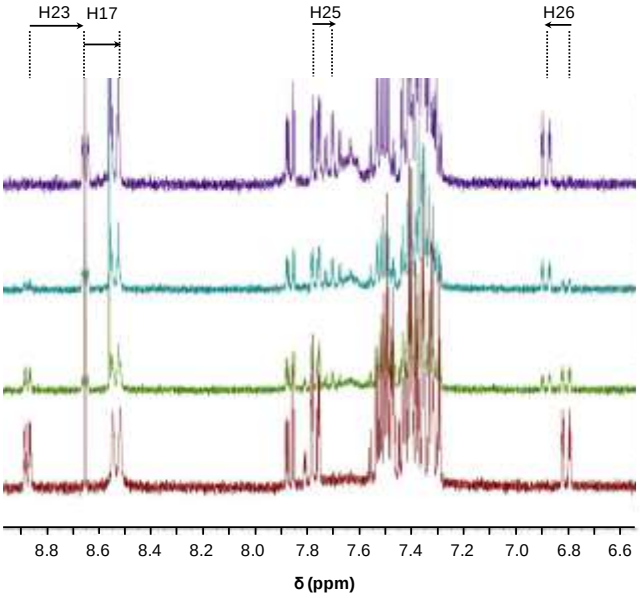

Fig. 6 Evolution of the ^{1}H NMR spectra of **1-TPP** in CD_3CN (~2.3×10^{-3} M) throughout photolysis at 350 nm *in situ* in the NMR tube. From bottom to top: t = 0, 3.5, 10 and 19 min irradiation. The dotted lines indicate the centres of multiplets and the arrows indicate the sense of variation of the chemical shifts during photolysis. See Fig. S17† for proton numbering and more details concerning H25.

Photolysis was also followed through the evolution of the IR spectrum of **1-TPP** in acetonitrile (Fig. 7). The three peaks at 2041, 1954 and 1930 cm^{-1} corresponding to the three CO ligands of the starting complex disappeared progressively, while two peaks appeared at 1943 and 1869 cm^{-1}. The rest of the IR spectrum was not noticeably affected. This observation indicates that one CO molecule has been released.

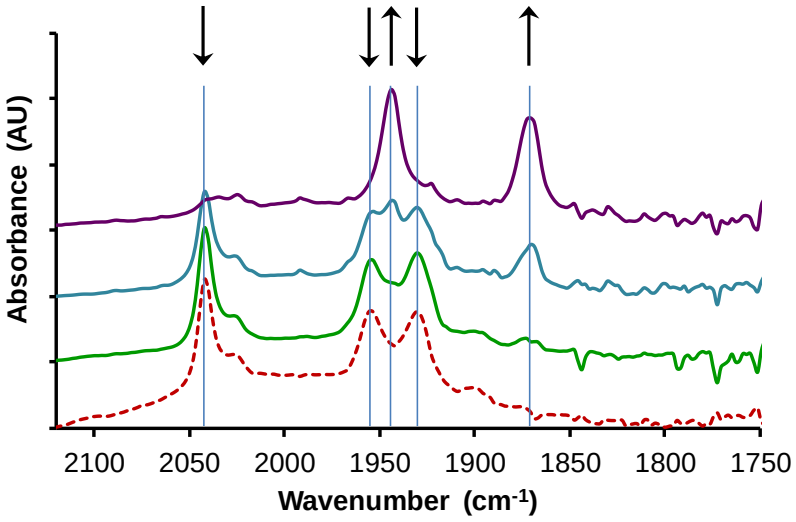

Fig. 7 Evolution of the FTIR spectrum of **1-TPP** in acetonitrile (9.9×10^{-4} M) throughout photolysis at 300 nm. From bottom to top: t = 0, 3, 8 and 13 min irradiation. The arrows indicate the sense of variations of the peak intensities during photolysis.

Finally, high resolution mass spectrometry of the photolyzed compound in positive mode showed a main peak at m/z 883, corresponding to the formula $C_{40}H_{28}N_5O_3P^{185}Re$, and a peak at m/z 842 that indicates to the loss of a CH_3CN molecule (Fig. S18†). No peak corresponding to the starting compound was detected, and the mass spectrum in negative mode was unchanged. This confirms the formation of the dicarbonyl solvento product $[Re(CO)_2(L)(PPh_3)(CH_3CN)]^+$ $CF_3SO_3^-$ (**2**) (see structure in Fig. S18†) upon photolysis.

Electronic properties

Calculations were made using the density functional theory (DFT) and time dependent density functional theory (TD-DFT) methods in order to get a better understanding of the spectroscopic and photochemical properties of the compounds. For complex **1-TPP** in acetonitrile, the bond lengths and angles calculated for the energy-minimized molecule at the S_0 ground state level were quite close to those obtained by X-ray diffraction (Table S1†), suggesting little geometry variation between solution and crystalline state. The HOMO-2 and HOMO-1 are distributed on the rhenium atom and on the carbonyl and phosphine ligands, the HOMO and LUMO+1 are almost exclusively centered on the PBO fragment, and the LUMO is localized on the pyta group (Table S3†, Fig. 8 and Fig. S19†). Data about higher energy orbitals is available in the ESI†. The HOMO-LUMO gap was significantly higher than that of the parent complex **1-Cl** (4.25 eV instead of 4.06 eV [17]). Regarding the first electronic transitions of **1-TPP**, calculations predict that the main contributor of the lowest energy band is a transition between HOMO-2 and LUMO (Table S4†) with mixed metal-to-ligand charge transfer (MLCT) and ligand-to-ligand charge transfer (LLCT) character, while the strong band at high energy results from the HOMO→LUMO+1 transition with intra ligand charge transfer (ILCT) character. Similarities can be noticed with the electronic structure of rhenium(I) tricarbonyl bipyridyl complexes with phosphine ligands,[27] which confirms that bipy and pyta ligands behave in much the same way. Very good agreement was found between the experimental and simulated absorption spectra (Fig. S20†). In the

first triplet state, orbitals are centered on the PBO moiety (Fig. S21†). For phosphorescence emission, the value predicted by DFT (601.9 nm) was relatively close to the experimental one, although the value predicted by TD-DFT (713.7 nm) was at too long wavelength (Table S6†).

Regarding photoproduct **2**, the cation $[Re(CO)_2(L)(PPh_3)(CH_3CN)]^+$ may theoretically exist as five isomers, depending on the position of the ligands with respect to each other. Calculations indicated that the isomer in which the acetonitrile ligand faces the phosphine group, specifically **2(iso1),** is the most stable (Fig. S22†). This result agrees well with studies first reported by Ishitani and co-workers, and subsequently confirmed by other groups, who provided strong evidence of selective photorelease of CO *trans* to the phosphorous ligand in closely related carbonyl complexes dissolved in coordinating solvents.[19,20,28] In fact, the phosphine group and the CO group *trans* to it strongly compete for the same metal orbitals, so that metal-to-CO π-backbonding is reduced, which favours preferential labilization of this CO group.

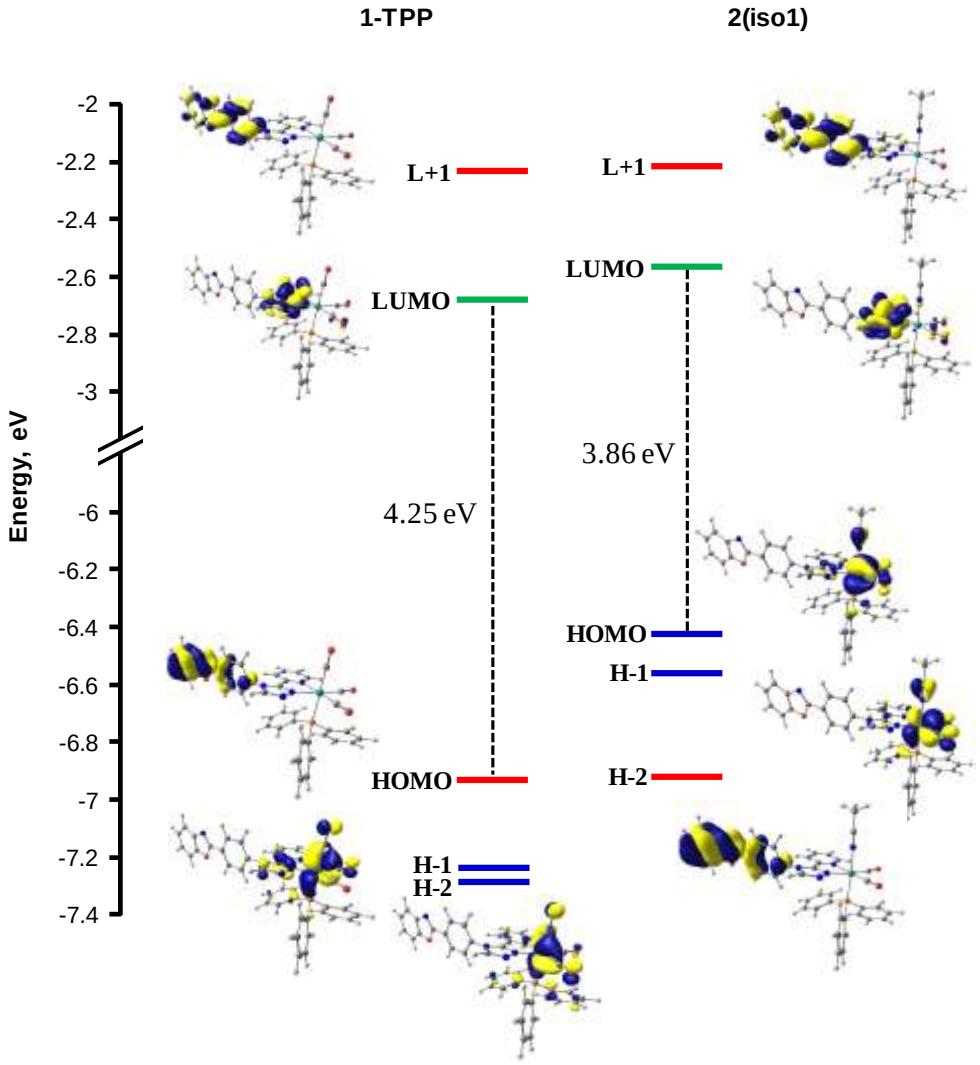

Fig. 8 Isodensity plots of selected frontier molecular orbitals involved in the first electronic transitions for the cation of complex **1-TPP** (left) and cation **2(iso1)** (right) in acetonitrile, according to TD-DFT calculations at the PBE1PBE/LANL2DZ/6-31+G** level of theory. Orbitals mainly centred on PBO (red line), Re and CO (blue line), and pyta (green line).

The calculated geometry of the photoproduct cation **2(iso1)** (Table S7†), as well as the composition and shape of molecular orbitals (Fig. 9, Table S8† and Fig. S23†), were quite close to those of **1**, with the striking difference that the HOMO and HOMO-2 were interchanged. As the result, the HOMO and HOMO-1 were mainly centred on the rhenium ion, while the HOMO-2 was centred on the PBO group. The transition between HOMO-1 and LUMO is mainly responsible for the MLCT band at long wavelength, while the HOMO-2→LUMO and HOMO-2→LUMO + 1 transitions generate the strong ILCT bands at short wavelengths (Table S9†). Again, the simulated UV-vis absorption spectrum fits very well with the experimental one (Fig. S20†). The orbital of the first triplet state is localized on the pyta group (Fig. S23†). Phosphorescence was expected slightly above 700 nm by both DFT and TD-DFT methods, quite close from the experimental value. The electronic structure of **2(iso1)** was reminiscent of the parent complex **1-Cl**, except that the HOMO-LUMO gap was smaller for **2(iso1)** (3.86 eV), which could favour non-radiative deactivation pathways and reduce phosphorescence efficiency for this complex.[29] Figure S24† allows the nature of orbitals and the energy levels to be compared for the three complexes.

The photolability depends on the ability of the molecule to transfer the electron density from the M-CO bonding orbitals to another location of the ligand system upon photoactivation.[4] The composition of LUMO and LUMO+1 shows that the electron density is indeed very weak on rhenium and on the carbonyl groups for **1-TPP**, but this is also the case for **2(iso1)** and **1-Cl** (Tables S3† and S8†, and ref. 16). This approach is therefore not predictive of the photochemical behaviour. Actually, it is generally accepted for transition metal complexes that photoactivated dissociation results from populating a dissociative ligand field, metal-centered triplet excited state (^{3}MC), thermally accessible from the ^{3}MLCT state.[21,30,31] Exploration of the triplet potential energy surface is therefore key to the understanding of the photo-dissociative behaviour of these complexes, which mainly depends on the energy barrier between the ^{3}MLCT and ^{3}MC states [30] and on the probability of radiationless transitions between the lowest triplet state T_1 and the ground state S_0, as shown by Saita *et al*. on tricarbonylrhenium complexes.[18] In our case, the energy barrier between the ^{3}MLCT and ^{3}MC states should be very low for complex **1-TPP**. It would be instructive to study how much the energy of the ^{3}MLCT state can be lowered with respect to the ^{3}MC state while keeping some photolability.[21] Finally, it is noteworthy that contrary to other rhenium complexes, **1-TPP** was photolyzed more efficiently by exciting in the MLCT band than in the ILCT band. It can be thought that populating high-energy excited states leads to a waste of energy in alternative photophysical processes.

CONCLUSIONS

In this work, it was shown that complex **1-TPP** acts as a single CO-donating photoCORM under the present photolysis conditions. Replacing the chloride ancillary ligand of **1-Cl** by a triphenylphosphine unit bestowed the complex with noticeable photoreactivity. Comparison with closely related molecules reported in the literature is not easy. The apparent rate of CO release k_{CO} is a very useful value to compare the reactivity of a set of compounds in the same study, but it depends on the irradiation device. Photoreactivity quantum yields are not systematically reported, and very strong variations can be found for the same complexes depending on the authors,[13,15,19] suggesting that the experimental conditions play an important role. Indeed, the present work confirmed that photoreactivity strongly depends on the

presence or absence of oxygen in solution, as well as on the excitation wavelength. Variations must also be expected with the nature of solvent. The photoreactivity quantum yield of **1-TPP** (0.10) in undegassed acetonitrile compares favourably with the values reported by Marker *et al.* (0.011 to 0.055) for Re(I) photoCORMs incorporating a phenanthroline or bipyridine bidendate ligand in undegassed aqueous solutions.[15] The value in degassed acetonitrile (0.29) is also higher than those reported by Pierri *et al.*[13] and by Koike *et al.*[19] for various complexes based on $[Re(bpy)(CO)_3(PR_3)]^+$ in similar medium, with the exception of the triphenylphosphine derivative whose photoreactivity quantum yield reaches 0.55.[19] The efficiency of CO production of **1-TPP** in degassed acetonitrile is only slightly lower than that reported for some Mn photoCORMs in organic solution,[32,33] and certainly significantly lower than that of the best Mn photoCORM.[25] The reason is probably that the heavy metal of **1-TPP** leads to strong spin-orbit interactions and to the dissipation of the excitation energy, instead of CO dissociation.[7-9]

In conclusion, among Re(I) complexes, **1-TPP** shows valuable photoreactivity and advantage may be taken from the marked changes observed in phosphorescence emission for monitoring the CO-production. The complex is very weakly soluble in water. At concentrations in the 10^{-5} M range, it forms stable aggregates that retain good photoreactivity. Irradiation in the near UV and in the violet region of the visible spectrum makes **1-TPP** not very well suited for direct use in living cells. Nonetheless, this complex is an interesting candidate for use in photoCORM materials. It could be incorporated as a photoactive agent into an optical fiber device for remote-controlled delivery of CO [34] or a cell culture substrate for therapeutic applications.[35] Work is also in progress to develop some new complexes that could be excited at longer wavelengths in the visible range.

EXPERIMENTAL SECTION

General methods. Analytical grade solvents were used without further purification for synthesis. For spectroscopy and photochemistry, HPLC grade solvents were used. Silver triflate and triphenylphosphine were from Acros Organics. Complex $[Re(CO)_3(L)(Cl)]$ (**1-Cl**) was prepared according to our previously reported method.[17] Analytical thin layer chromatography (TLC) and chromatography purification were respectively conducted using Kieselgel 60 F254 and neutral alumina from Merck. NMR, mass and infrared spectra were obtained in the relevant 'Services communs de l'Institut de Chimie de Toulouse, Université de Toulouse III-Paul-Sabatier'. ^{1}H- and ^{13}C-NMR spectra were recorded using a Bruker Avance 300 spectrometer operating at 300 MHz for ^{1}H and 75 MHz for ^{13}C. Chemical shifts are reported in ppm, with residual protonated solvents as internal references. Attributions of the signals were made using 2D NMR data (COSY, HSQC and HMBC) (Fig. S1 to S10†). NMR numbering scheme are given in Fig. S1† and Fig. S17†. App = Apparent; * = The multiplicity of the signal is more complex as it is part of an AA′XX′ system. Electrospray (ESI) mass spectra and High-Resolution Mass Spectra (HRMS) were obtained on a QTRAP Applied Biosystems spectrometer and on a Xevo G2 QTof Waters spectrometer, respectively. Infrared spectra were obtained on a Nexus Thermonicolet apparatus with DTGS as the detector. Microcrystals were observed using a Zeiss Axioskop fluorescence microscope equipped with an Andor Luca camera, in transmission mode. The excitation wavelength was 435–450 nm.

Synthesis

$[Re(CO)_3(L)(CH_3CN)]^+(CF_3SO_3)^-$. In a vessel placed under nitrogen atmosphere and protected from light, complex $[Re(CO)_3(L)(Cl)]$ (**1-Cl**) (100 mg, 0.16 mmol), silver trifluoromethanesulfonate (60 mg, 0.23 mmol) dissolved in acetonitrile (20 mL) and tetrahydrofuran (2 mL) were heated overnight at 90°C. After cooling, the solution was filtered off on sintered glass, and then filtered twice on a 0.45 µm-PTFE Millipore® and once on a 0.22 µm-GF-Millipore®. The solvents were evaporated, giving a yellow powder (120 mg) which was used with no further purification. Yield = 91%.

^{1}H NMR (300 MHz, CD_3CN) δ (ppm) = 9.08 (ddd, *J* = 5.5, 1.6, 0.8 Hz, 1H, H23), 8.75 (s, 1H, H17), 8.57 (app. d*, *J* = 8.9 Hz, 2H, H11, H15), 8.01 (td, *J* = 7.9, 1.5 Hz, 1H, H25), 7.88 (app. d*, *J* = 8.7 Hz, 2H, H12, H14), 7.87 – 7.82 (m, 1H, H4), 7.78 – 7.73 (m, 1H, H7), 7.69 (ddd, *J* = 7.9, 5.5, 1.3 Hz, 1H, H24), 7.51 – 7.47 (m, 2H, H5, H6), 7.35 (td, *J* = 8.3, 1.2 Hz, 1H, H26), 2.15 (s, 3H, CH_3). ^{13}C NMR (75 MHz, CD_3CN) δ (ppm) = 194.86 (CO), 193.89 (CO), 190.37 (CO), 162.2 (C2), 156.7 (C20), 156.6 (C23), 151.8 (C9), 148.9 (C17), 145.7 (C21), 142.7 (C8), 142.1 (C25), 135.3 (C13), 131.1 (C10), 130.4 (C11, C15), 129.8 (C24), 128.7 (C12, C14), 127.1 (C5), 126.1 (C6), 124.8 (C26), 123.5 (CN), 121.1 (C4), 111.9 (C7), 4.0 (CH_3). HRMS-ESI$^-$: *m/z* 148.9520 ($[M]^-$ calcd for CF_3O_3S, 148.9520). HRMS-ESI$^+$: *m/z* 649.0780 ($[M]^+$ (100 %) calcd for $C_{25}H_{16}N_6O_4{}^{185}Re$, 649.0763), 608.0515 ($[M - CH_3CN]^+$ (25%) calcd for $C_{23}H_{13}N_5O_4{}^{185}Re$, 608.0874), 681.1042 ($[M + CH_3OH]^+$ (29%) calcd for $C_{26}H_{19}N_6O_5{}^{185}Re$, 681.1025).

$[Re(CO)_3(L)(PPh_3)]^+(CF_3SO_3)^-$, complex 1-TTP. In a vessel placed under nitrogen atmosphere and protected from light, complex $[Re(CO)_3(L)(CH_3CN)]^+(CF_3SO_3)^-$ (120 mg, 0.15 mmol) and triphenylphosphine (393 mg, 1.5 mmol) dissolved in tetrahydrofuran (20 mL) were heated overnight at 70°C. After cooling, pentane (20 mL) was added dropwise to precipitate PPh_3. After filtration, the filtrate was concentrated (3 mL) by evaporating part of the solvent under reduced pressure, and diethyl ether was added. The precipitated product was collected and rinsed with ether in a soxhlet for 4h to give an orange powder (68 mg). Yield = 45%. For very high purity, the compound was subsequently purified by chromatography on alumina using an eluent system ranging from pure ethyl acetate to ethyl acetate/methanol 96:4 v/v. Yield = 30 %.
^{1}H NMR (300 MHz, CD_3CN) δ (ppm) = 8.88-8.82 (m, 1H, H23), 8.65 (s, 1H, H17), 8.51 (app. d*, *J* = 9.3 Hz, 2H, H11, H15), 7.86-7.82 (m, 1H, H4), 7.81-7.71 (m, 2H, H25, H7), 7.53-7.43 (m, 8H, H5, H6, H12, H14, H24, H30), 7.42-7.26 (m, 12H, H28, H29), 6.81-6.78 (m, 1H, H26). ^{13}C NMR (75 MHz, CD_3CN) δ(ppm) = 195.74 (d, $J_{C\text{-}P}$ = 10.1 Hz, CO), 194.97 (d, $J_{C\text{-}P}$ = 10.5 Hz, CO), 185.48 (d, $J_{C\text{-}P}$ = 5.6 Hz, CO), 162.1 (C2), 156.7 (C23), 155.2 (C20), 151.9 (C8), 148.9 (C17), 144.5 (C21), 142.8 (C9), 141.3 (C25), 134.7 (C10), 134.15 (d, $J_{C\text{-}P}$ = 10.8 Hz, C28), 132.1 (d, $J_{C\text{-}P}$ = 2.3 Hz, C30), 131.3 (C13), 130.4 (C11), 130.0 (d, $J_{C\text{-}P}$ = 10.0 Hz, C29), 129.85 (C24), 129.80 (d, $J_{C\text{-}P}$ = 46.3 Hz, C27), 128.6 (C12), 127.2 (C5), 126.1 (C6), 124.7 (C26), 121.2 (C4), 111.9 (C7). HRMS-ESI$^-$: *m/z* 148.9519 ($[M]^-$ calcd for CF_3O_3S, 148.9520); HRMS- ESI$^+$: *m/z* 870.1407 ($[M]^+$ calcd for $C_{41}H_{28}N_5O_4P^{185}Re$, 870.1408). IR(ATR): ν(CO) = 2044, 1957, 1910 cm^{-1}.

X-ray crystallography. Crystal data were collected at 253 K on a Bruker AXS Quazar APEX II diffractometer using a 30 W air-cooled microfocus source (ImS) with focusing multilayer optics using MoKα radiation (wavelength = 0.71073 Å). Phi- and omega-scans were used. The structure was solved using intrinsic phasing method (ShelXT).[36] All non-hydrogen atoms were refined anisotropically using the least-square method on F^2.[37] Solvent molecule was disordered. Several restraints (SAME, SIMU, DELU) were applied to refine this molecule and to avoid the collapse of the structure during the least-squares refinement by the large anisotropic displacement parameters.

Empirical formula: $C_{41}H_{28}N_5O_4PRe$, CF_3O_3S, $CHCl_3$; Formula weight: 1140.29; Crystal system: triclinic; Space group: $P\ \bar{1}$; Unit cell dimensions: a = 12.9001(9) Å, b = 14.1290(9) Å, c = 14.1372(10) Å, α = 68.331(2)°, β = 77.247(2)°, γ = 71.348(2)°; V: 2253.4(3) Å^3; Z = 2; Density (calculated): 1.681 Mg/m^3; Crystal size: 0.260×0.040×0.040 mm^3; Reflections collected/Independent: 67667/9181; [R(int)=0.0994]; Data/restraints/parameters: 9181/132/614; Final R1 indices [I>2σ(I)] = 0.0423; wR2 (all data) = 0.1017; Largest diff. peak and hole: 0.832 and -0.992 e.Å^{-3}. Supplementary crystallographic data for CCDC-2019719 can be obtained free of charge from The Cambridge Crystallographic Data Centre via https://www.ccdc.cam.ac.uk/structures/.

Computational details. The GAUSSIAN09 program package [38] was employed for all calculations (the geometry optimization, the ground-state and excited-state electronic structures, and optical spectra) with the aid of the ChemCraft visualization program.[39] The ground state (S_0), the first excited state (S_1) and the lowest triplet state (T_1) geometries of compounds were fully optimized with the restricted and unrestricted density functional theory (R-DFT and U-DFT) method using the Perdew-Burke-Ernzerhof PBE1PBE functional without symmetry constraints.[40] In all calculations, the "double-ζ" quality basis set LANL2DZ with Hay and Wadt's relative effective core potential ECP (outer-core [($5s^25p^6$)] electrons and the ($5d^6$) valence electrons) [41,42] was employed for the Re atom. The 6-31+G** basis set for H, C, N, O, P and Cl atoms was used.[43] The solvent effect (acetonitrile, ε = 35.688) was simulated using the Self-Consistent Reaction Field (SCRF) under the Polarizable Continuum Model (PCM).[44,45] The vibrational frequencies calculations were performed using the optimized structural parameters of compounds, to confirm that each optimized structure represents a local minimum on the potential energy surface and all eigenvalues are non-negative. On the basis of the optimized ground and excited state geometries, the absorption and emission properties were calculated by the time dependent density functional theory (TD-DFT) method at the PBE1PBE/LANL2DZ/6-31+G** level. These methods have already shown good agreement with experimental studies for different rhenium(I) complexes.[46]

Spectroscopy. The solutions of complex **1-TPP** were prepared by gentle heating in a solvent, sonication and filtration on paper filter prior to measurement. When not specified, solutions were not degassed. Degassed solutions were bubbled with argon for 5 minutes before measurement. Spectroscopic measurements in solutions were conducted at 20°C in a temperature-controlled cell. UV-visible absorption spectra were recorded on a Hewlett Packard 8453 spectrometer. Fluorescence spectra of solutions were measured with a Xenius SAFAS spectrofluorometer using cells of 1 cm optical pathway and were corrected. The fluorescence quantum yields (Φ_F) were determined using the classical formula:

$$\Phi_{Fx} = (A_s \times F_x \times n_x^2 \times \Phi_{Fs})/(A_x \times F_s \times n_s^2) \quad (1)$$

where A is the absorbance at the excitation wavelength, F the area under the fluorescence curve and n the refraction index. Subscripts s and x refer to the standard and to the sample of unknown quantum yield, respectively. Coumarin 153 (Φ_F = 0.53) in ethanol was used as the standard.[47] The absorbance of the solutions was equal or below 0.055 at the excitation wavelength. The error on the quantum yield values is estimated to be about 10 %.

Phosphorescence decay curves in dilute acetonitrile (Abs at λ_{ex}< 0.1) were recorded using the time-correlated single-photon counting method (TCSPC) on a Fluorolog 3-2(iHR320) spectrofluorimeter equipped with a nanoled-370 (λ_{ex}=371 nm). Emitted photons were detected at 90° through a monochromator by means of a Hamamatsu R928 photomultiplier. Emission was recorded near the maximum with a bandpass of 10-15 nm. The instrumental response was recorded directly on the sample at 635 nm before each decay curve. All analyzes were recorded using the Datastation v2.7 software. The decay curves were analyzed with reconvolution and global non-linear least-squares minimization method using DAS6 v6.8 software.

The solid state spectrum was recorded on a Xenius SAFAS spectrofluorometer equipped with a $BaSO_4$ integrating sphere and corrected using a home-made correction curve. Solid samples were deposited on a metal support and luminescence spectra were corrected. The absolute photoluminescence quantum yield values (Φ_P) were determined by a method based on the one developed by de Mello *et al.*,[48] as described elsewhere.[16] The error was estimated to be about 20%.

Photochemistry. Unless specified, dye solutions were non-degassed. For monitoring by ^{1}H NMR spectroscopy, solutions were directly irradiated in NMR tubes. In all other case, they were placed in fluorescence 1 cm × 1cm quartz cuvettes. Irradiation was performed using a Rayonet reactor equipped with lamps emitting at 350 or 300 nm. The photochemical rate constant k was measured by monitoring the rise of absorbance at 402 nm following exposure to UV light for various time intervals ranging between 0 to 120 s. The k value was then calculated from the ln(a-x) value vs time (t) plot. ln(a-x) = ln a[1-(A_t-A_0)/(A_F-A_0)], with a: initial concentration of **1-TPP**, x: concentration of formed product, A: absorbance at 402 nm before reaction (A_0), at time t (A_t) and at t =180 s (A_F).

To determine the photoreaction quantum yield of **1TPP** for irradiation at 350 nm, the number of photons X received by the sample was first measured using potassium ferrioxalate actinometry, according to a variant of the method described by Hatchard and Parker.[49] The photodecomposition of potassium ferrioxalate is commonly evaluated by complexation of the ferrous ions produced with 1,10-phenanthroline, leading to a strongly-coloured red complex. Solutions were prepared with minimal light exposure and stored in the dark. A 3 mL volume (V_1) of potassium ferrioxalate (6.1 mM) in 0.1N H_2SO_4 was placed in a 1 cm × 1 cm quartz cell and irradiated for 1 min under magnetic stirring. After irradiation, an aliquot of 150 µL (V_2) was added to a mixture of 3 mL 1,10-phenanthroline (5.7 mM in 0.1N H_2SO_4) and 75 µL sodium acetate buffer (1.8 M, pH5) (V3 = 3.225 mL). The resulting mixture was left to stand in the dark under gentle stirring for 30 min, and then absorbance was measured. Blank was made according to the same procedure using non-irradiated potassium ferrioxalate solution. The number of photons received by the sample was determined using the equation:

$$X = (\Delta A V_1 V_3 N_A)/(1000 \Phi \varepsilon V_2 t l) \quad (2)$$

where ΔA is the change in absorbance at 510 nm of the mixture, N_A is Avogadro's number, Φ is the quantum yield (~1.25) of ferrioxalate at 350 nm, ε is the extinction coefficient of the 1,10-phenanthroline/Fe^{2+} complex at 510 nm (~11000 $M^{-1}cm^{-1}$), t is the irradiation time and l is the optical

path length. The average of four measurements resulted in a photon number of 3.6×10^{16} photon.s^{-1}. In a second phase, an aliquot (3 mL) of an acetonitrile solution of **1TPP** at 4.3×10^{-4} M was irradiated at 350 nm1 in a 1 cm × 1 cm quartz cell. The absorbance at 350 nm was above 2.5, ensuring that all photons were absorbed by the sample. After a short period of irradiation time resulting in no more than 10% photolysis, absorbance at 402 nm was measured. The extinction coefficient of the photoproduct was determined after complete photolysis, allowing the number of molecules of photoproduct formed to be calculated. The photoreaction quantum yield was calculated as the ratio of photoproduct molecules to the number of absorbed photons determined by the ferrioxalate actinometry.

ASSOCIATED CONTENT

Supporting Information

Molecular views, additional computational, spectroscopic and photochemical data.

CONFLICTS OF INTEREST

There are no conflicts to declare.

ACKNOWLEDGEMENTS

A. D. H. M. thanks the International Research Experiences for Undergraduates UF/France iREU: NSF Award CHE-1659782 and NIH Research Initiative for Scientific Enhancement (RISE) program of UPR-Río Piedras: Grant No. 5R25GM061151-17. All authors are grateful to Dr. Corinne Routaboul (Service commun de spectroscopie infrarouge, ICT) for the measurement of FTIR spectra, Dr. Charles-Louis Serpentini (IMRCP) for the measurement of phosphorescence lifetimes, and to Ms. Fernanda Conçalvez (SPCMIB) for the study of stability in solutions. The calculations were carried out in the Wroclaw Centre for Networking and Supercomputing, Poland (http://www.wcss.pl).

Keywords: Photochemistry; Phosphorescence; Crystal; Rhenium; Transition metal complex; Carbon monoxide

REFERENCES

[1] R. Motterlini and L. E. Otterbein, *Nat. Rev. Drug. Discovery*, 2010, **9**, 728–743.

[2] S. H. Heinemann, T. Hoshi, M. Westerhausend and A. Schiller, *Chem. Commun*., 2014, **50**, 3644–3660.

[3] M. A. Gonzales and P. K. Mascharak, *J. Inorg. Biochem*., 2014, **133**, 127–135.

[4] M. A. Wright and J. A. Wright, *Dalton Trans.*, 2016, **45**, 6801–6811.

[5] E. Kottelat and F. Zobi, *Inorganics*, 2017, **5**, 24-1/24-19.

[6] J. Marhenke, K. Trevino and C. Works, *Coord. Chem. Rev.*, 2016, **306** (Part 2), 533–543.

[7] I. Chakraborty, S. J. Carrington and P. K. Mascharak, *Acc. Chem. Res.*, 2014, **47**, 2603−2611.

[8] I. Chakraborty, S. J. Carrington, G. Roseman and P. K. Mascharak, *Inorg. Chem.*, 2017, **56**, 1534−1545.

[9] I. Chakraborty, S. J. Carrington and P. K. Mascharak, *ChemMedChem*, 2014, **9**, 1266–1274.

[10] L. C.-C. Lee, K.-K. Leung and K. K.-W. Lo, *Dalton Trans.*, 2017, **46**, 16357–16380.

[11] K. K.-W. Lo, *Acc. Chem. Res*. 2015, **48**, 2985−2995.

[12] I. Chakraborty, J. Jimenez, W. M. C. Sameera, M. Kato and P. K. Mascharak, *Inorg. Chem.*, 2017, **56**, 2863–2873.
[13] A. E. Pierri, A. Pallaoro, G. Wu and P. C. Ford, *J. Am. Chem. Soc.*, 2012, **134**, 18197–18200.
[14] S. J. Carrington, I. Chakraborty, J. M. L. Bernard and P. K. Mascharak, *Inorg. Chem.*, 2016, **55**, 7852−7858.
[15] S. C. Marker, S. N. MacMillan, W. R. Zipfel, Z. Li, P. C. Ford and J. J. Wilson, *Inorg. Chem.*, 2018, **57**, 1311–1331.
[16] J. Wang, B. Delavaux-Nicot, M. Wolff, S. Mallet-Ladeira, R. Métivier, E. Benoist and S. Fery-Forgues, *Dalton Trans.*, 2018, **47**, 8087–8099.
[17] J. Wang, A. Poirot, B. Delavaux-Nicot, M. Wolff, S. Mallet-Ladeira, J. P. Calupitan, C. Allain, E. Benoist and S. Fery-Forgues, *Dalton Trans.*, 2019, **48**, 15906–15916.
[18] K. Saita, Y. Harabuchi, T. Taketsugu, O. Ishitani and S. Maeda, *Phys. Chem. Chem. Phys.*, 2016, **18**, 17557–17564.
[19] K. Koike, N. Okoshi, H. Hori, K. Takeuchi, O. Ishitani, H. Tsubaki, I. P. Clark, M. W. George, F. P. A. Johnson and J. J. Turner, *J. Am. Chem. Soc.*, 2002, **124**, 11448–11455.
[20] K. Koike, J. Tanabe, S. Toyama, H. Tsubaki, K. Sakamoto, J. R. Westwell, F. P. A. Johnson, H. Hori, H. Saitoh and O. Ishitani, *Inorg. Chem.*, 2000, **39**, 2777–2783.
[21] A. E. Pierri, P.-J. Huang, J. V. Garcia, J. G. Stanfill, M. Chui, G. Wu, N. Zheng and P. C. Ford, *Chem. Commun.*, 2015, **51**, 2072–2075.
[22] A. François, C. Auzanneau, V. Le Morvan, C. Galaup, H. S. Godfrey, L. Marty, A. Boulay, M. Artigau, B. M. Voegtlé, N. Leygue, C. Picard, Y. Coulais, J. Robert and E. Benoist, *Dalton Trans.*, 2014, **43**, 439–450.
[23] M. R. Gonçalves and K. P.M. Frin, *Polyhedron*, 2017, **132**, 20–27.
[24] R. A. Kirgan, B. P. Sullivan and D. P. Rillema, *Top. Curr. Chem.*, 2007, **281**, 45–100.
[25] S. J. Carrington, I. Chakraborty and P. K. Mascharak, *Dalton Trans*., 2015, **44**, 13828–13834.
[26] C. Carayon and S. Fery-Forgues, *Photochem. Photobiol. Sci.*, 2017, **16**, 1020−1035, and refs therein.
[27] F. Zhao, J. Wang, W. Liu, Y. Wang, *Comput. Theor. Chem*., 2012, **985**, 90–96.
[28] I. Chakraborty, S. J. Carrington, J. Hauser, S. R. J. Oliver and P. K. Mascharak, *Chem. Mater.*, 2015, **27**, 8387−8397.
[29] J. S. Wilson, N. Chawdhury, M. R. A. Al-Mandhary, M. Younus, M. S. Khan, P. R. Raithby, A. Köhler and R. H. Friend, *J. Am. Chem. Soc.*, 2001, **123**, 9412–9417.
[30] K. Nisbett, Y.-J. Tu, C. Turro, J. J. Kodanko and H. B. Schlegel, *Inorg. Chem.*, 2018, **57**, 231−240, and refs therein.
[31] E. J. Baerends and A. Rosa, *Coord. Chem. Rev.*, 1998, **177**, 97–125.
[32] M. A. Gonzalez, S. J. Carrington, N. L. Fry, J. L. Martinez, and P. K. Mascharak, *Inorg. Chem*., 2012, **51**, 11930−11940.
[33] J. Jimenez, I. Chakraborty, A. Dominguez, J. Martinez-Gonzalez, W. M. Chamil Sameera, and P. K. Mascharak, *Inorg. Chem.* 2018, **57**, 1766−1773.
[34] S. Gläser, R. Mede, H. Görls, S. Seupel, C. Bohlender, R. Wyrwa, S. Schirmer, S. Dochow, G. U. Reddy, J. Popp, M. Westerhausen and A. Schiller, *Dalton Trans*., 2016, **45**, 13222–13233.
[35] S. Diring, A. Carné-Sánchez, J.-C. Zhang, S. Ikemura, C. Kim, H. Inaba, S. Kitagawa and S. Furukawa, *Chem. Sci.*, 2017, **8**, 2381–2386.
[36] G. M. Sheldrick, *Acta Cryst. A*, 2015, **71**, 3–8.
[37] G. M. Sheldrick, *Acta Cryst. C*, 2015, **71**, 3–8.

[38] M. J. Frisch, G. W. Trucks, H. B. Schlegel, G. E. Scuseria, M. A. Robb, J. R. Cheeseman, G. Scalmani, V. Barone, B. Mennucci, G. A. Petersson, H. Nakatsuji, M. Caricato, X. Li, H. P. Hratchian, A. F. Izmaylov, J. Bloino, G. Zheng, J. L. Sonnenberg, M. Hada, M. Ehara, K. Toyota, R. Fukuda, J. Hasegawa, M. Ishida, T. Nakajima, Y. Honda, O. Kitao, H. Nakai, T. Vreven, J.A. Montgomery, J.E. Peralta, F. Ogliaro, M. Bearpark, J. J. Heyd, E. Brothers, K. N. Kudin, V. N. Staroverov, R. Kobayashi, J. Normand, K. Raghavachari, A. Rendell, J. C. Burant, S. S. Iyengar, J. Tomasi, M. Cossi, N. Rega, J. M. Millam, M. Klene, J. E. Knox, J. B. Cross, V. Bakken, C. Adamo, J. Jaramillo, R. Gomperts, R. E. Stratmann, O. Yazyev, A. J. Austin, R. Cammi, C. Pomelli, J. W. Ochterski, R. L. Martin, K. Morokuma, V. G. Zakrzewski, G. A. Voth, P. Salvador, J. J. Dannenberg, S. Dapprich, A. D. Daniels, O. Farkas, J. B. Foresman, J.V. Ortiz, J. Cioslowski and D. J. Fox, *Gaussian 09, Revision A.1*, Gaussian, Inc., Wallingford CT, 2009.

[39] G. Zhurko and D. Zhurko, ChemCraft 1.6, 2011, http://www.chemcraftprog.com/index.html

[40] J. P. Perdew, K. Burke and M. Ernzerhof, *Phys. Rev. Lett.* 1996, **77**, 3865–3868.

[41] P. J. Hay and W. R. Wadt, *J. Chem. Phys.* 1985, **82**, 270–283.

[42] P. J. Hay, W. R. Wadt, *J. Chem. Phys.* 1985, **82**, 299–310.

[43] W. J. Hehre, L. Radom, P. V. R. Schleyer and J. A. Pople, *Ab initio Molecular Orbital Theory*, Wiley, New York, 1986.

[44] B. Mennucci and J. Tomasi, *J. Chem. Phys.* 1997, **106**, 5151–2158.

[45] M. Cossi, V. Barone, B. Mennucci and J. Tomasi, *Chem. Phys. Lett.* 1998, **286**, 253–260.

[46] G. Velmurugan, B. K. Ramamoorthi and P. Venuvanalingam, *Phys. Chem. Chem. Phys.* 2014, **16**, 21157–21171.

[47] K. Suzuki, A. Kobayashi, S. Kaneko, K. Takehira, T. Yoshihara, H. Ishida, Y. Shiina, S. Oishi and S. Tobita, *Phys. Chem. Chem. Phys*. 2009, **11**, 9850–9860.

[48] J. C. De Mello, H. F. Wittmann and R. H. Friend, *Adv. Mater.* 1997, **9**, 230–232.

[49] C. G. Hatchard and C. A. Parker, *Proc. R. Soc. Lond. A* 1956, **235**, 518–536.